Dalton Transactions

Accepted Manuscript

ROYAL SOCIETY OF CHEMISTRY

www.rsc.org/dalton

Self-Assembly of Tri-Pyrazolate Linked Cages with Di-Palladium Coordination Motifs

Xuan-Feng Jiang, [a, b] *Wei Deng,* [b] *Rui Jin,* [b] *Lin Qin,* [b] *Shu-Yan Yu* [*a, b]

[a]Beijing Key Laboratory for Green Catalysis and Separation, Department of Chemistry and Chemical Industry, College of Environmental and Energy Engineering, Beijing University of Technology, Beijing 100124, P.R. China.

[b]Laboratory for Self-Assembly Chemistry, Department of Chemistry, Renmin University of China, Beijing 100872, China.

To whom correspondence should be addressed. E-mail: yusy@ruc.edu.cn.

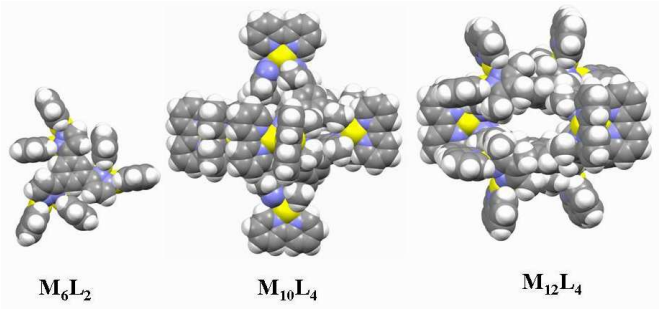

Abstract

By employing di-palladium complexes $[(N^N)_2Pd_2(NO_3^-)_2](NO_3^-)_2$ (where N^N = 2, 2′-bipyridine, bpy; 4, 4′-dimethylbipyridine, dmbpy; 1,10-phenanthroline, phen) as corners and tripyrazole functional ligands (H_3L^1~ H_3L^5) as linkers, a series of high-positively-charged tripyrazolate-bridged metallo-cages with different conformation and cavity such as $[Pd_6L_2]^{6+}$ (**1** or **5**, where L = L^1 or L^5), $[Pd_{10}L^2{}_4]^{10+}$ (**2a,**

2b and **4b**, where L = L^2 or L^4) and $[Pd_{12}L_4]^{12+}$ (**3** or **4a**, where L= L^3 or L^4), have been synthesized through a di-metal coordination directed self-assembly with spontaneous deprotonation of the tripyrazole ligands in aqueous solution. These complexes have been fully characterized by ^1H and ^{13}C NMR, cold-spray ionization or electron spray ionization mass spectrometry (CSI-MS, ESI-MS) and elemental analysis. Complexes **1, 2a, 2b, 3** and **4** have also been determined by single-crystal X-ray diffraction structural analysis. In the case of complex **3**, six PF_6^- anions were encapsulated within the cavity composing of adjacent di-Pd corners.

Introduction

The coordination chemistry of polynuclear transition metals has attracted a considerable current interest because of their unusual structures and catalytic, optical, photochemical, electronic and magnetic properties.[1-5] Pyrazoles as a class of versatile nitrogen-donor ligands with variable coordination modes play an important role in inorganic, organometallic and materials chemistry[6] and could also be used to construct pyrazolate-bridged multi-metal and metal-metal bonding coordination systems.[7] Therefore, the coordination chemistry of pyrazoles and of its derivatives received particular attention because of not only their structural beauty and diversity such as metal-based polymers,[8] metallo-macrocycles, metallo-cages and so on,[7,15] but also because of their broad application prospects and relevance in multimetal-centered catalysis,[8] biological mimicry,[9] magnetic coupling,[10] multielectron-transfer reaction,[11] photophysical studies,[12] and so forth.[13,14]

In view of the variety of potential applications of pyrazolate-bridged multi-metal coordination macrocyclic and cage-like hosts, we have devoted our great efforts to develop the self-assembly of metallo-macrocycles with bi- or poly-pyrazolate-bridged ligands.[16] Such metal-organic macrocycles have shown promise for the complexation of anions and small organic molecules in water.[15-17] Since 2005, we have reported a new kind of bipyrazolate linked metallo-macrocycles with dimetal clips $[(N\hat{}N)_2M_2(NO_3)_2](NO_3)_2$ (M = Pd or Pt)[18] through spontaneous deprotonation of the 1*H*-bipyrazole

ligands. Along this line, we have developed the solution self-assembly of tripyrazolate trianion linkers with coordinated dimetallic clips leads to the formation of $Pd_{12}L_4$ cages with interior cavities.[17]

Herein, we designed and used five tri-pyrazolyl ligands (H_3L^1 – H_3L^5) with different sizes as linkers and dimetallic clips[17] $[(N^N)_2Pd_2(NO_3^-)_2](NO_3^-)_2$ as corners to self-assembly a series of metallo-macrocyclic cage complexes **1** – **5** (as shown in Scheme 1 – 3) via a directed self-assembly approach that involves spontaneous deprotonation of the 1*H*-bipyrazolyl ligands in aqueous solution. In particular, the versatile assembling linker pyrazolyls were introduced on the backbone of aromatic groups adopting tripodal conformation *via* multi-step synthesis (Scheme 4). These new tri-pyrazole derivatives (Figure 1) that are capable of constructing rich self-assembling motifs regarding hydrogen bonding, metal coordination may give rise to more fascinating supramolecular architectures (Figure 2). Utility of such poly-pyrazole ligands and di-palladium motifs lead to form three types of metal-organic supramolecular architectures including dimeric cage $[Pd_6L_2] \bullet 6NO_3^-$ (**1**• $6NO_3^-$, L=L^1 ; **5** • $6NO_3^-$, L=L^5), metallo-macrocycles $[Pd_{10}L_4] \bullet 10NO_3^-$ (**2a** and **2b** • $10NO_3^-$, L=L^3; **4b** • $10NO_3^-$, L=L^4) and $[Pd_{12}L_4] \bullet 12NO_3^-$ (**3**•$12NO_3^-$**,** L=L^3 or **4a**•$12NO_3^-$, L=L^4), respectively. All the compounds present here were characterized by ^1H and ^{13}C NMR, CSI or ESI mass spectroscopies, Elemental analysis and in some cases by X-ray single crystal diffraction analysis.

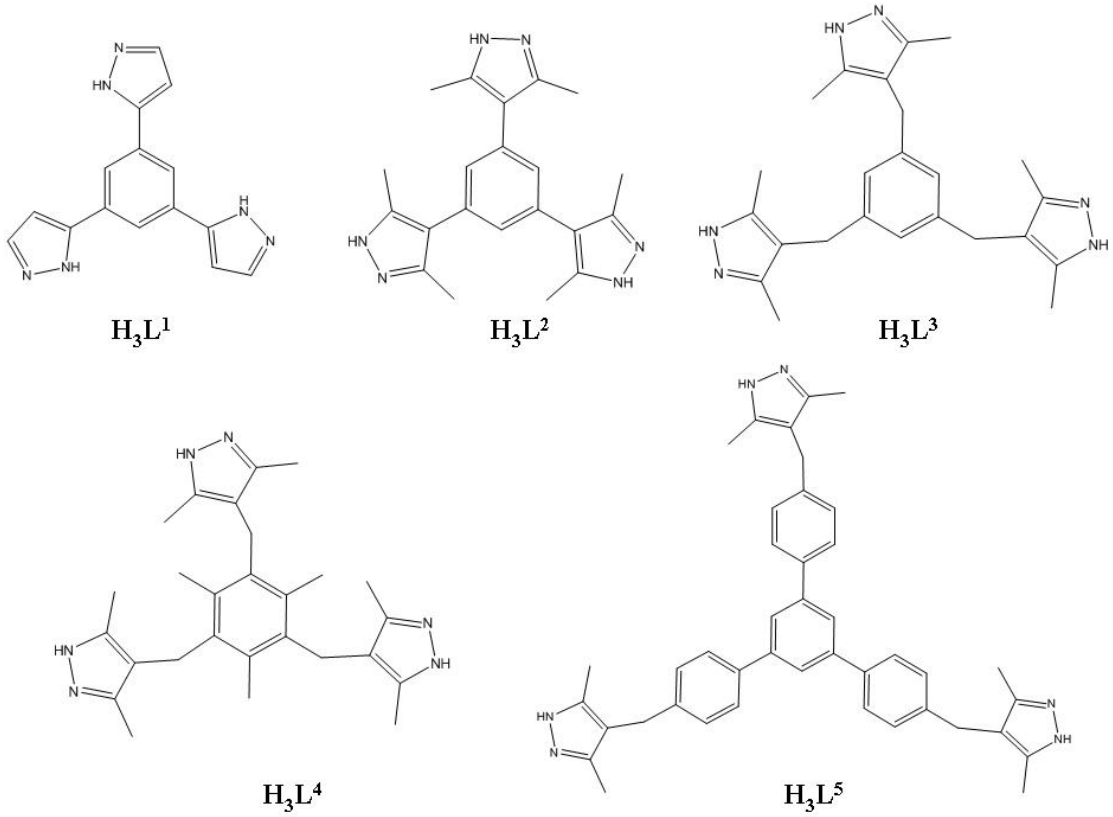

Figure 1. The structures of the flexible and rigid tripyrazole ligands H_3L^1-H_3L^5

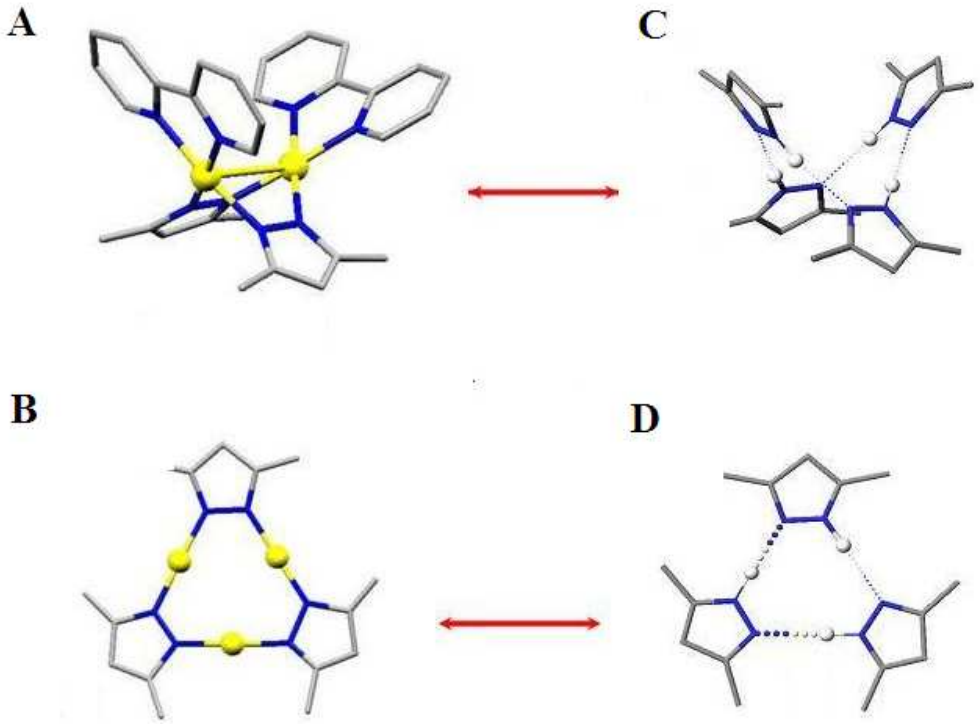

Figure 2. The self-assembling motifs constructed from polypyrazolate ligands. Yellow balls represent

metal atom， M = Pd(II), Pt(II), (A)； M = Cu(I), Ag(I), Au(I), (B and D); pale balls represent hydrogen atom (C).

Result and Discussion

Synthesis of Tri-pyrazolate Ligands. Figure 1 presents all the tripyrazole ligands employed in this work. The ligands H_3L^1 ~ H_3L^3 were synthesized according to the published procedures.[21] The other ligands H_3L^4 ~ H_3L^5 were synthesized according to the reported methods similar to that used for the known pyrazolate ligands.[15-16]

Self-Assembly and Characterization of the $[Pd_6L_2]^{6+}$-Type Cages. Combination the dimetal corners $[(bpy)_2Pd_2(NO_3)_2](NO_3)_2$ with 0.33 equivalent of H_2L (H_2L^1 or H_2L^5) in aqueous solution at room temperature (as shown in scheme 1). The resulting mixture was heated for 24 hrs, leading to the formation of hexanuclear cages $\{[(bpy)_2Pd_2]_3L_2]\}$ $\bullet(NO_3^-)_6$ (**1** or **5**, where L=L^1 or L^5) in high yield with spontaneous deprotonation of tri-pyrazolate ligands.

Cage **1** was fully characterized by elemental analysis, NMR spectroscopies, CSI-TOF-MS and X-ray crystal structure determination. The ^1H and ^{13}C NMR analysis of the product confirmed the formation of a single highly symmetrical species, and integration of the signals indicated 3:1 ratio of dimetal motifs $[(bpy)_2Pd_2(NO_3^-)_2](NO_3^-)_2$ to the tripyrazolate trianion L^1 in the cage **1** (Figure 3). Remarkably, the signals corresponding to the coordinated bpy ligands present two sets of triplets at 8.48, 7.84 and one multiplet at 8.43 ~ 8.32 ppm in the downfield region of the spectrum, and the resonances of the tripyrazolate trianions L^1 were found at 7.85, 7.34, 7.15 ppm. The formation of the **[**$Pd_6L_2]^{6+}$-type cage was further supported by cold spray ionization mass spectrometry (CSI-MS):[19] 1350.3，852.2，602.7, 453.3 and 353.5 for $[\mathbf{1} \bullet 4PF_6^-]^{2+}$, $[\mathbf{1} \bullet 3PF_6^-]^{3+}$, $[\mathbf{1} \bullet 2PF_6^-]^{4+}$, $[\mathbf{1} \bullet PF_6^-]^{5+}$ and $[\mathbf{1}]^{6+}$ (Figure 4).

Scheme 1. Self-assembly of $[Pd_6L_2]^{6+}$-Type Cage (where L = L^1, L^5)

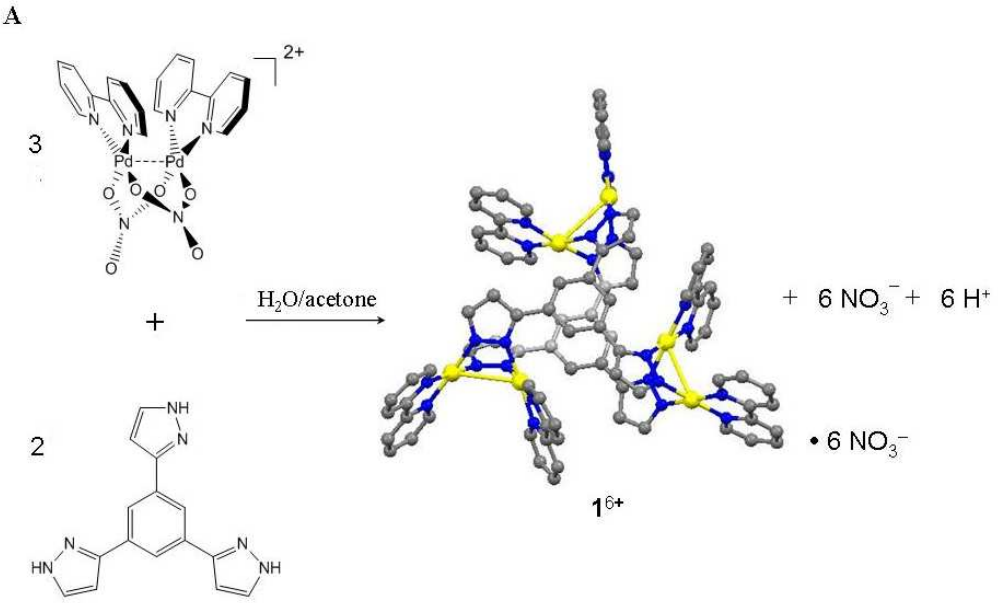

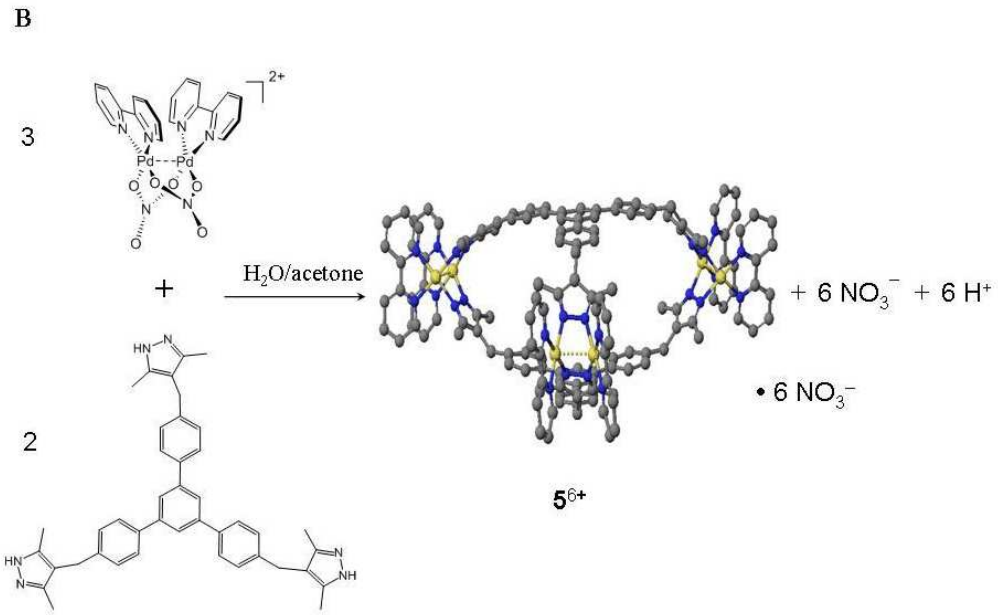

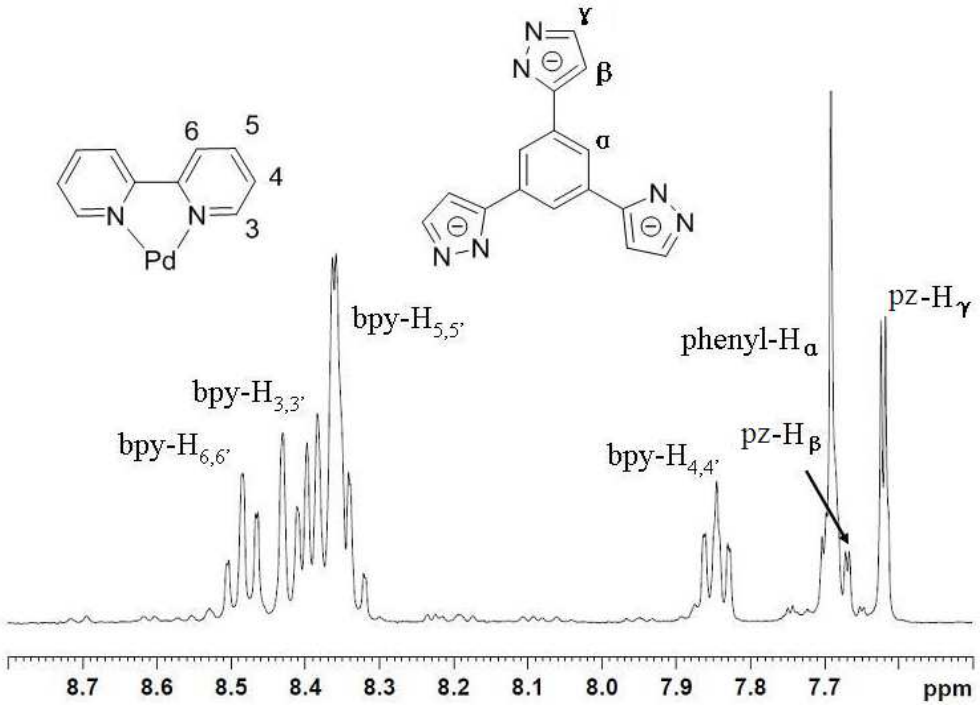

Figure 3. ^{1}H NMR spectra of **1**•6PF_6^- (400M Hz, CD_3CN, 25℃, TMS).

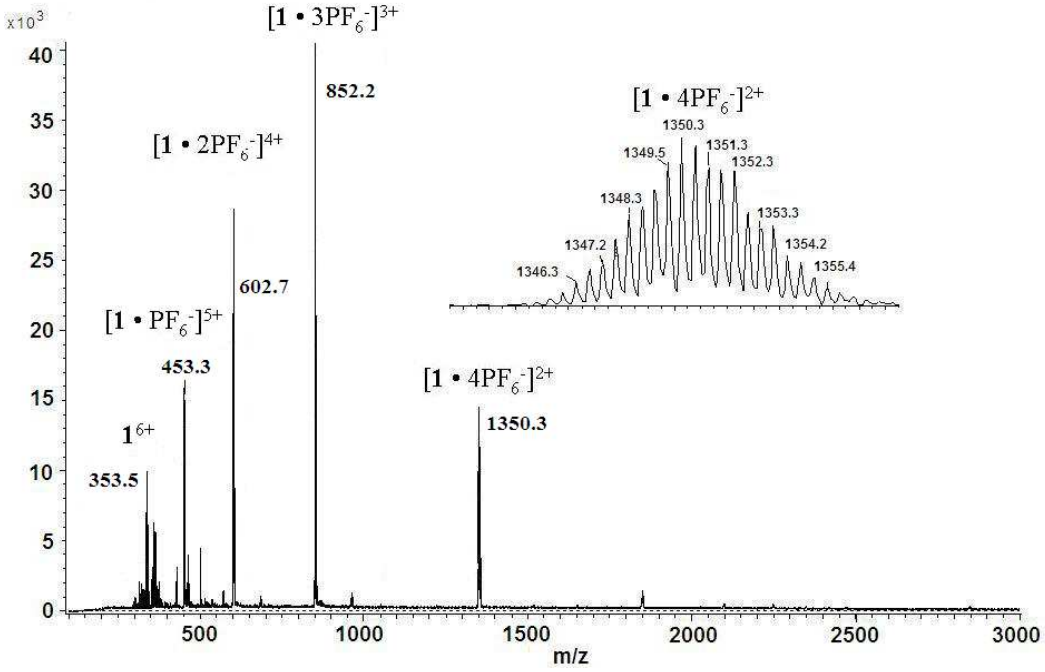

Figure 4. CSI-TOF-MS spectra of **1** • 6PF_6^- in acetonitrile; the inset shows the isotopic distribution of the species [**1** • 4PF_6^-]$^{2+}$.

Similar synthetic method for preparation of **1** was used to synthesize complex **5** except that the flexible tripod ligands H_3L^5 (Scheme 1B). On the basis of the ^{1}H NMR spectra, complex **5** possessed a

symmetric structure. As shown in the Figure 5，the chemical shifts at 7.45 and 7.36 ppm were attributed to protons of the phenyl-H from tripyrazole L^3 and protons of the bpy moieties shown four sets of signals at 8.84, 8.43, 8.67 and 8.09 ppm. Moreover, the NMR spectrum of **5** evidently confirmed that a complex of molar ratio 3:1 (bpy)Pd to L^3 is isolated. Notably, one singlet at 2.75 ppm, ascribed to the methyl protons of the tripyrazole ligand L^3 is evident in the upfield region of the spectrum. The formation of the $[Pd_6L_2]^{6+}$-type-metallomacrocyclic structure was further supported by ESI-MS in acetonitrile as illustrated in Figure 6, the mass to charge ratio (m/z) peaks 1090.3、586.2 and 472.7 for $[\mathbf{5} \cdot 3PF_6^-]^{3+}$, $[\mathbf{5} \cdot PF_6^-]^{5+}$ and $[\mathbf{5}]^{6+}$.

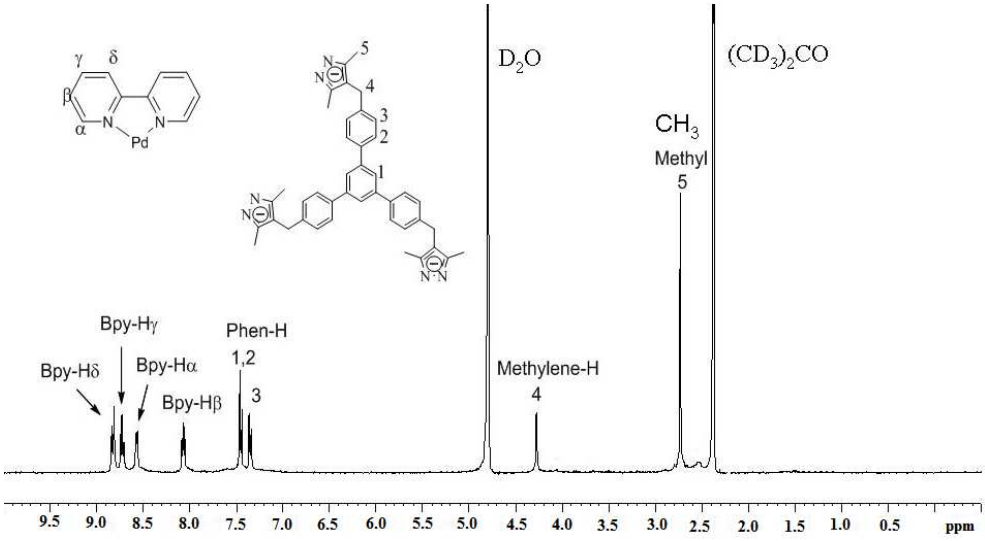

Figure 5. ^{1}H NMR spectra of **5** • $6PF_6^-$ (400M Hz, CD_3CN, 25℃, TMS).

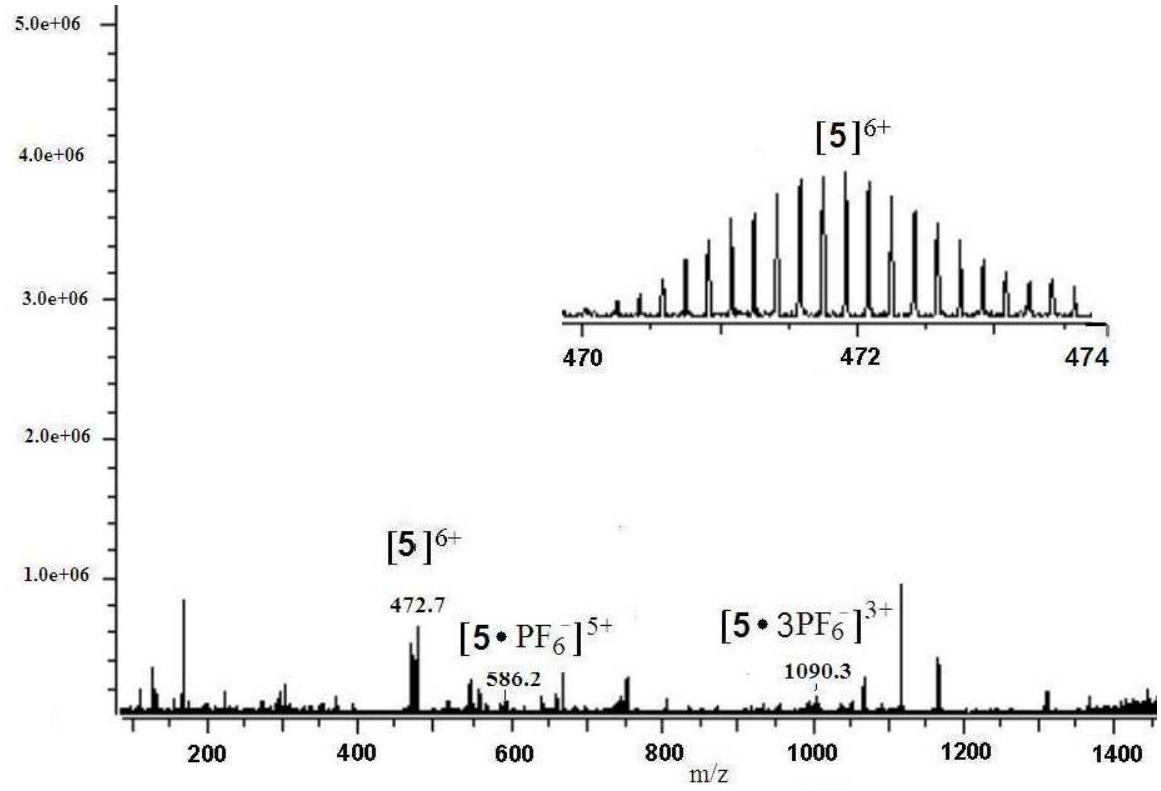

Figure 6. ESI-MS spectra of **5** • $6PF_6^-$ in acetonitrile; the inset shows the isotopic distribution of the species $[\mathbf{5}]^{6+}$.

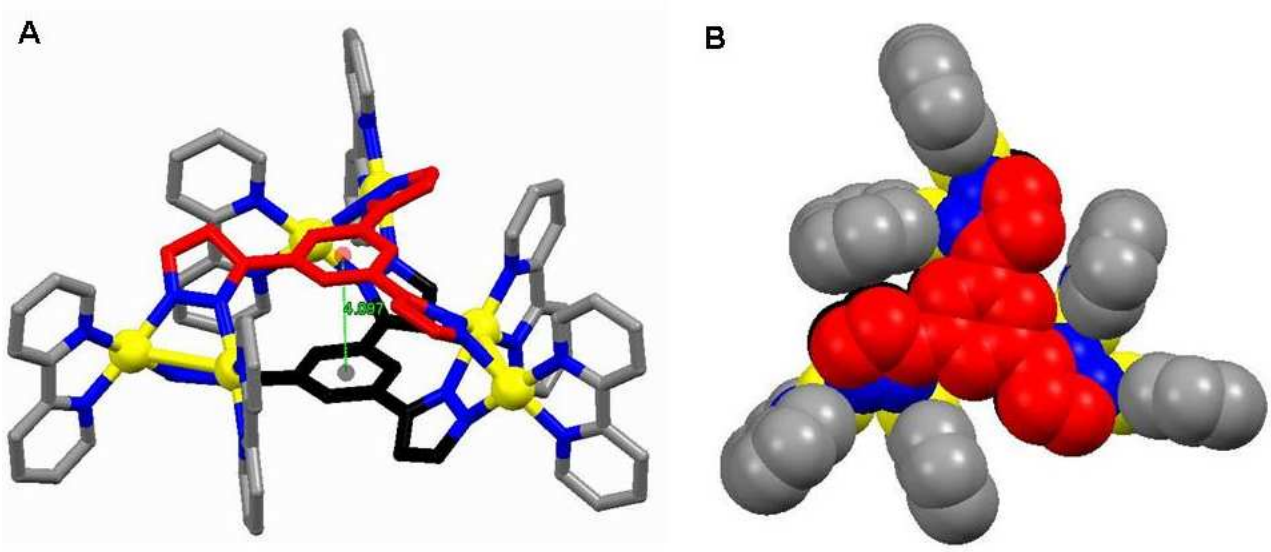

Figure 7. The molecular structure of **1** • $6NO_3^-$. The counterions, hydrogen atoms and solvent molecules are omitted for clarity. (A, side view drawn in the ball and stick mode; B, top view drawn in the spacefill mode. Yellow balls represent metal atom Pd (II); gray balls represent carbon atom).

Crystal Structure of the $[Pd_6L^1_2]^{6+}$-Type Cage 1. The high symmetric cage-like structure of complex

1 was supported by single-crystal structure analysis.[25] The crystal structure of **1** • $6NO_3^-$ was shown in Figure 7, complex **1** • $6NO_3^-$ crystallizes in the triclinic space group *P-1*. The crystal structure analysis for **1** reveals the Pd_6 dimeric cage-shaped structure with three (μ-pyrazolato-N, N′)$_2$ doubly-bridged $[(bpy)Pd]_2$ dimetal corners. In the dimeric cage, two tripyrazole ligands L^1 coordinated with six (bpy)Pd motifs and resulting the formation of $[Pd_6L_2]$-Type cage with a centra distance of 4.086 Å between adjacent phenyl rings from tripyrazole. Two phenyl rings are almost coplanar, and each one form a dihedral angle of about 36.02^o with pyrazole planes in the tripyrazole bridged ligand, shown a *syn*, *syn, syn* orientation according to the planes of (bpy)Pd1 and (bpy)Pd2. Three dimetal motifs $[(bpy)_2Pd_2(pz)_2]^{2+}$ arranged in the propeller-like fashion. The separations of Pd1···Pd2, Pd3···Pd4 and Pd5···Pd6 are 3.118, 3.173 and 3.071 Å (see SI Table S2), respectively, suggesting the presence of weak metal-metal interactions. The dihedral angle between the two pyrazolate (N18-N19 and N22-N23; N10-N11 and N14-N15) planes at each corner are 69.99^o, 73.12^o and 62.04^o, respectively, which are smaller than the dihedral angle between the bpy ligands (about 106.91^o).

Self-Assembly and Characterization of the $[Pd_{10}L_4]^{10+}$-Type Cage. Treatment the dimetal corners $[(bpy)_2Pd_2(NO_3^-)_2](NO_3^-)_2$ with a solution containing 0.33 equivalent of H_3L^2 in 1:1 H_2O–acetone at room temperature (as shown in scheme 2). The resulting mixture was heated for 48 hrs, leading to the formation of $[Pd_{10}L^2_4](NO_3^-)_{10}$ (complex **2a**) with spontaneous deprotonation of tripyrazolate ligands. The pure complex **2a** as light yellow microcrystalline solid were obtained by the evaporation of solution at room temperature. Complex **2a** was fully characterized by elemental analysis, NMR spectroscopy, ESI-MS and X-ray crystal structure determination. The ^{1}H and ^{13}C NMR analysis of the product confirmed the formation of a single asymmetrical species, and integration of the signals indicates 10:4 ratio of dimetal motifs $[(bpy)_2Pd_2(NO_3^-)_2](NO_3^-)_2$ to the tripyrazolate trianion L^2 in the complex **2a** (Figure S12 and S13). Remarkably, the signals corresponding to the coordinated bpy ligands present two multiplets at 8.78~8.35 ppm, 7.91~7.62 ppm in the downfield region of the spectrum, respectively. The resonances of the tripyrazolate trianions L^2 were splitted into three signals observed at 7.45 ppm,

6.74 ppm, 6.31 ppm. Meanwhile, the proton signals of methylene groups contained three sets of doublets (1.61, 2.43, 2.79 ppm), this splitting was affected by the high distortion of methylene groups between the phenyl ring and pyrazolate group. The formation of the **[**$Pd_{10}L^2_4]^{10+}$-type cage was further supported by electron spray ionization mass spectrometry (ESI-MS):[19] 1107.6，873.1 and 717.6 for [**2a** • $6NO_3^-]^{4+}$, [**2a** • 5 $NO_3^-]^{5+}$ and [**2a** • $4NO_3^-]^{6+}$ (Figure S14).

Scheme 2. Self-assembly of $[Pd_{10}L^2_4]^{10+}$-Type Metallo-Macrocycle

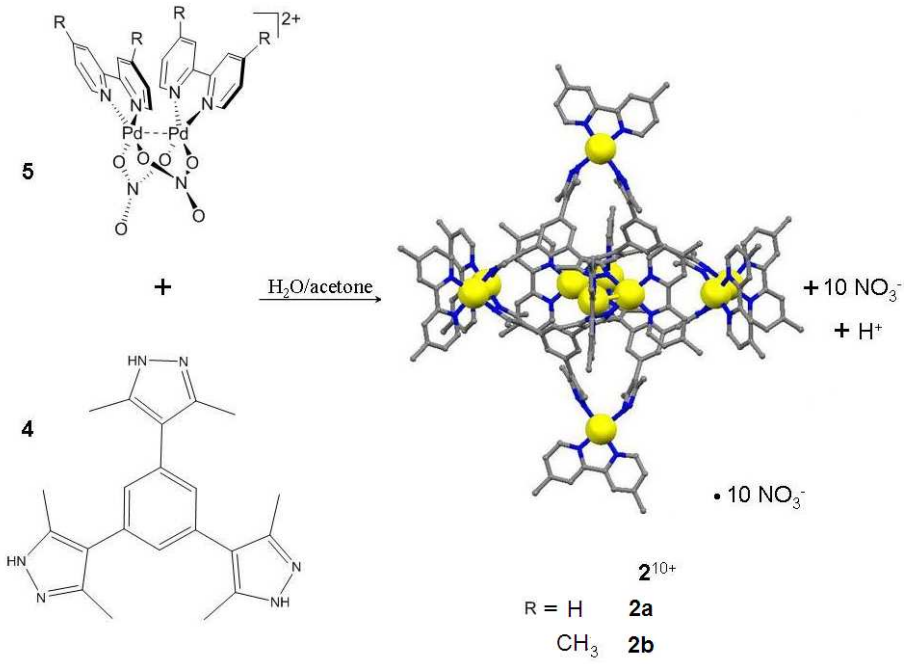

Crystal Structure of $[Pd_{10}L^2_4]^{10+}$-Type Metallo-Macrocycle. The X-ray single crystal determination was successfully used to collect high-quality data. The crystallography revealed that disordered, amorphous solvent molecules and counter ions existing in the target structure of **2a**•$10NO_3^-$, which presented a $[Pd_{10}L^2_4]$ metal-organic macrocyclic architecture with four (μ-pyrazolato-N,N′)$_2$ doubly bridged $[(bpy)_2Pd_2(pz)_2]^{2+}$ (where pz = pyrazolate anion) dimetal coordination motifs and two single metal corners $[(bpy)Pd(pz)_2]^{2+}$ (Figure 8). Inversion centre existing in the crystallographic asymmetric unit indicated that the structure of **2a**•$10NO_3^-$ was low symmetry. Four tripyrazolate anionic linkers (L^2) coordinated to four $[(bpy)_2Pd_2]^{2+}$ dimetal corners and two monometallic motifs, leading to the formation of metallomacrocycle $[Pd_{10}L^2_4]$•$10NO_3^-$ (**2a**•$10NO_3^-$). The molecular dimensions are

approximately 13 Å × 13 Å × 19 Å. Due to the self-assembling reactions occurred in the water environment, strong amphiphilic interaction force the hydrophobic organic ligands to arrange toward the inside of metallomacrocycle with high positive charge, the highly ionized hydrophilic dimetal coordination motifs were outside of the macrocycle. In the metallomacrocycle, each tripyrazolate linkers adopted distorted conformation to coordinate with $[(bpy)_2Pd_2]_2^{2+}$ corners. The dihedral angles between three pyrazolyl and backbone aromatic group are 56.22°, 42.23° and 51.01°, respectively. Two pyrazolate groups located at the 1 and 3-position of linker L^2 were locked by $[(bpy)_2Pd_2(pz)_2]^{2+}$ coordination motifs, resulting in the formation of $[Pd_4L^2_2]$ macrocyclic subunits bearing two intermolecular dimetal coordination motifs with Pd···Pd distances of 3.182 to 3.215 Å within the $[Pd_{10}L^2_4]$ macrocyclic tetramer **2a**. The distance between two Pd(II) atoms (Pd1 to Pd4) is 9.94 Å. The central distance between the phenyl groups from two tripyrazolate linkers is 7.498 Å in the $[Pd_4L^2_2]$ subunit. Two $[Pd_4L^2_2]$ macrocyclic subunits were hold together through two pyrazolate groups locating at the 5-position bridging-coordinate with single metal $[(bpy)Pd]^{2+}$ corners, finally leading to the construction of trimacrocyclic cage $[Pd_{10}L^2_4]^{10+}$. The similar structure **2b** was successfully obtained in the same method (Figure S32).

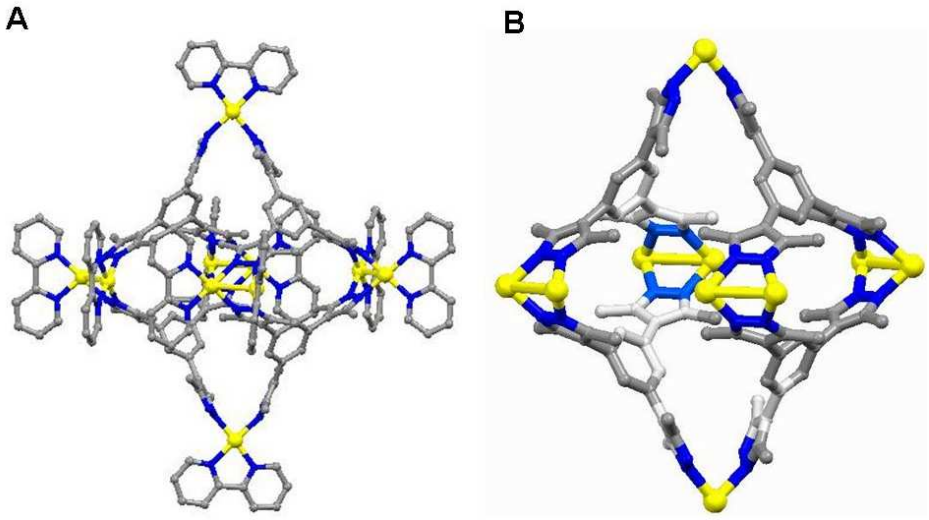

Figure 8. The crystal structure of macrotricyclic cage **2a**, All NO_3^- anions, hydrogen atoms (A) and 2, 2′-bipy groups (B) were omitted for clarity. Yellow, Pd (II); gray, C; blue, N).

Self-Assembly and Characterization of the $[Pd_{12}L_4]^{12+}$-Type Cage (where L= L^3 and L^4). In a similar fashion, cage **3** was prepared by the reaction of flexible tripyrazolate ligands H_3L^3 and the dimetal corners $[(phen)_2Pd_2(NO_3)_2](NO_3)_2$ in a 1 : 3 ratio in water at room temperature lead to the self-assembly of the macrotricyclic cage $\{[(phen)Pd]_{12}L^3{}_4\}(NO_3)_{12}$ (**3** • $12NO_3^-$) in quantitative yield (Scheme 2A).[16] The PF_6^- salt of **3** was obtained as yellow microcrystals in quantitative yield. As shown in Figure S18 and S19, the ^{1}H NMR spectrum of **3** • $12PF_6^-$ revealed the formation of 3:1 dimetal clip to tripz ligand complex. The signals of the tripyrazolate L^2 were observed at 7.66, 5.79 ppm, and protons of phenanthroline (phen) ligand shown at 8.87, 8.78, 8.38, 8.18, 8.11 and 7.95 ppm. Two sets of signals appearing at 4.01 and 3.87 ppm were ascribed to the protons of methylene groups connecting Pz and aromatic group (Ar-*CH*$_2$-Pz). The proton signals of methylene located at 3 and 5- position of pyrazolate groups (Pz-*CH*$_3$) contained four sets of singlets appearing at 2.71, 2.25 and 2.02 ppm, which caused by the high distortion of methylene groups between the aromatic ring and pyrazolyl group. ESI-MS spectra of **3** in acetonitrile solution allowed the clear assignment of the $[Pd_{12}(phen)_{12}L^3{}_4]$ • 12 PF_6^- compositions (Figure S20). For example, multiply charged molecular ions of **3** at m/z = 1209.8 [**3** • $7PF_6^-]^{5+}$, 984.5 [**3** • $6PF_6^-]^{6+}$, 823.0 [**3** • $5PF_6^-]^{7+}$, 702.1 [**3** • $4PF_6^-]^{8+}$, 608.0 [**3** • $3PF_6^-]^{9+}$ were observed.

Similar method was used to synthesis complex **4a**. The ^{1}H and ^{13}C NMR spectra indicated the formation of a single species. As shown in the Figure S22, ^{1}H NMR spectroscopy of **4a** • 12 PF_6^- clearly revealed a discrete array of well-defined resonance and all of the chemical shifts in the spectrum could be respectively ascribed to three kinds of protons, namely bpy-H, methylene-H, phenyl-methyl-H and methyl-H. Notably, the integrations of two nonequivalent protons of above each group are present in a 2:1 ratio in the self-assembly product, which are marked with blue and red arrows in the spectra (e.g., for Methyl-H, δ = 2.8 and 3.2 ppm, for methylene-H, δ = 4.32, 4.08 , 3.82, 3.54, 3.33, 3.22 ppm, for phenyl-methyl-H, δ = 2.95, 2.68, 2.58 ppm). Related chemical shifts of the pyrazolyl groups drawn in blue and red in the ^{1}H-NMR spectrum are not equivalent. Such results were very similar to those observed in described-above macrotricyclic structure of complex **3** and indicated the low symmetric

geometry of **4a** induces two different chemical environments for the same kind of groups. The high distortion of methylene groups between the phenyl ring and pyrazolyl group caused the proton signals of methylene groups splitting into five sets of multiplets. This remarkable difference suggests that the presence of the dimetallic coordination clips restricts the mobility of pyrazolyl groups and increases the rigidity of the macrotricyclic framework. Although NMR considerations allowed us to tentatively propose the structure of macrotricyclic cage **4a**, the tentative structure was supported by CSI-MS for this complex. The CSI-MS spectra of **4a** • $12PF_6^-$ in acetonitrile showed two peaks corresponding to that of consecutive loss of PF_6^- counterions (Figure S23). The mass to charge ratio (m/z) peaks 1519.1 , 964.3 for [**4a** • $8PF_6^-$]$^{4+}$ and [**4a**• $6PF_6^-$]$^{6+}$, respectively, are in good agreement with theoretical values.

According to the data, complex **4a** should have the similar macrocyclic topology. Therefore, a visual molecular model was computed using CAChe program 6.1.1 to evaluate the size and conformation of macrocyclic cage **4a (**Figure 10).

Scheme 3. Self-assembly of $[Pd_{12}L^3_4]^{12+}$-type-metallo-macrocycle

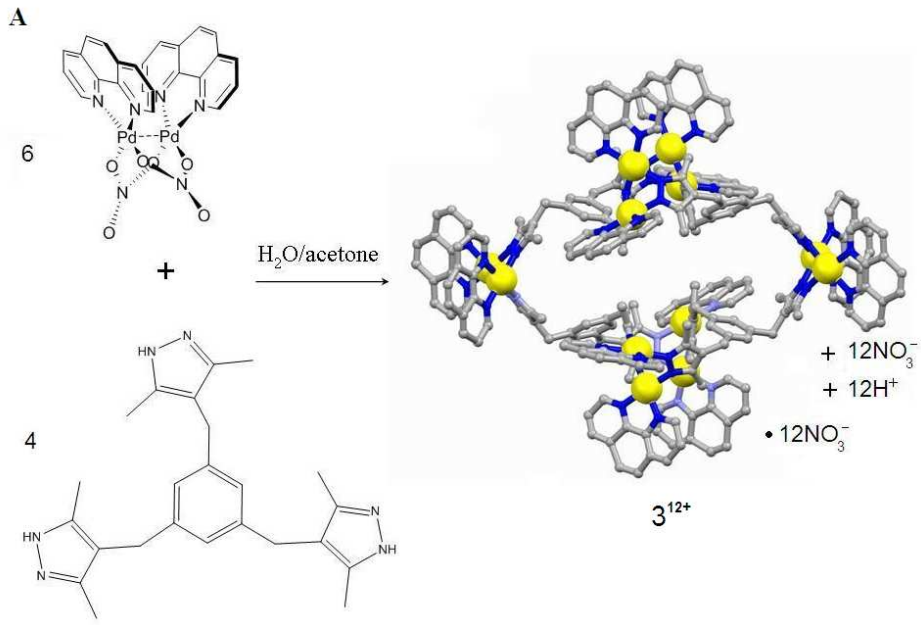

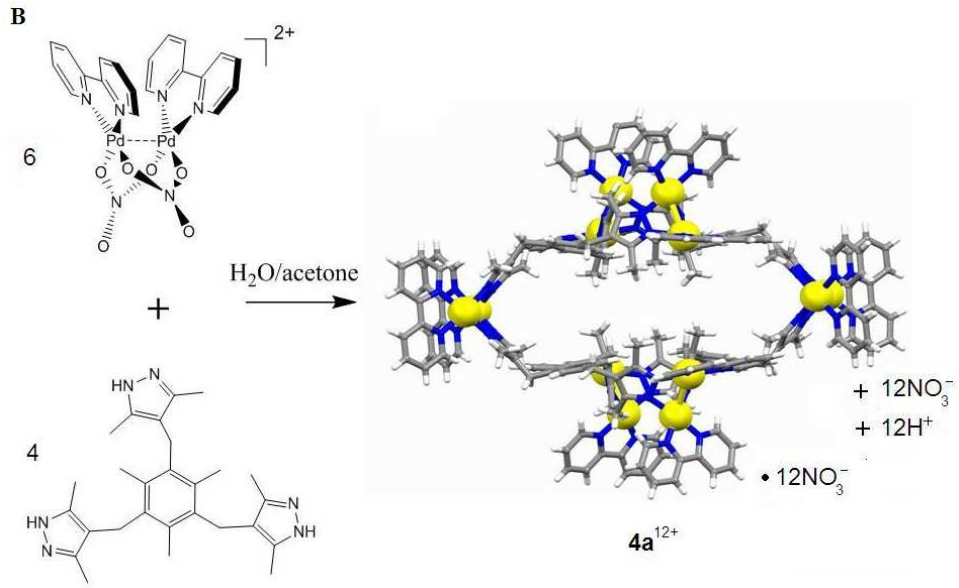

Crystal Structure of $[Pd_{12}L^3_4]^{12+}$-Type Metallo-macrocycle. Single crystals of **3**•12PF_6^- were obtained by vapor diffusion of diethyl ether into their acetonitrile solution. Complex **3**•12PF_6^- crystallizes in the triclinic space group *P*-1. The molecular dimensions are approximately 28 × 24 × 22 Å, and the dimensions of the inner cavity are roughly 20.2 × 11.6 × 8.6 Å as defined by the distance between adjacent dipalladium centers (as shown in the Figure 9). The interior void of about 1800 $Å^3$ is estimated. The crystal structure analysis for **3**•12PF_6^- revealed the macrotricyclic conformation with six (μ- pyrazolato-N, N′)$_2$ doubly bridged [(phen)Pd]$_2$ corners. Similar structure to cage **2** was also found in **3**, two pyrazolate groups located at the 1- and 3-position of linker L^3 were locked by two $[(phen)_2Pd_2(pz)_2]^{2+}$ coordination motifs, resulting in the formation of $[Pd_4L^3_2]$ macrocyclic subunits bearing two intermolecular dimetal coordination motifs within the $[Pd_{12}L^3_4]$-Type macrocyclic tetramer **3**. The dihedral angles between coordination planes of the Phen linkers are 87.31° (Pd1 and Pd2), 74.98° (Pd3 and Pd4), and 80.52° (Pd5 and Pd6), respectively. Because of the large dihedral angles, there are no π···π interactions between the Phen ligands coordination planes (Table S5). In the di-Pd(II) corners, the separations of Pd1···Pd2 (3.265 Å), (Pd3···Pd4) (3.204 Å), and Pd5···Pd6 (3.314 Å) are near the sum of van der Waals radii of palladium (the typical value is 1.6 Å), which shows quite weak Pd···Pd interaction. Six PF_6^- anions in the crystal are located outside the cavity and adjacent to the Phen

ligands by hydrogen bonds of C-H···F. Interestingly, it was also found that the macrotricyclic cages could pack into tubular channel with the wall containing the bridged linkers and the phen aromatic rings, which extended in the crystallographic *a*, *b*, and *c* axes with PF_6^- anions frozen inside.

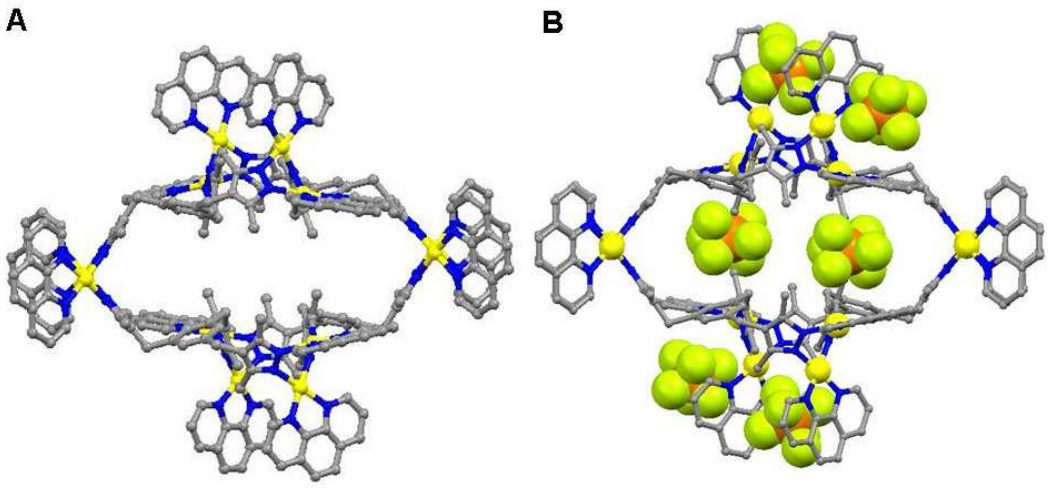

Figure 9. The crystal structure of macrotricyclic cage **3**•12PF_6, A) without anions and B) with anions. (Yellow, Pd (II); gray, C; blue, N; light green, F).

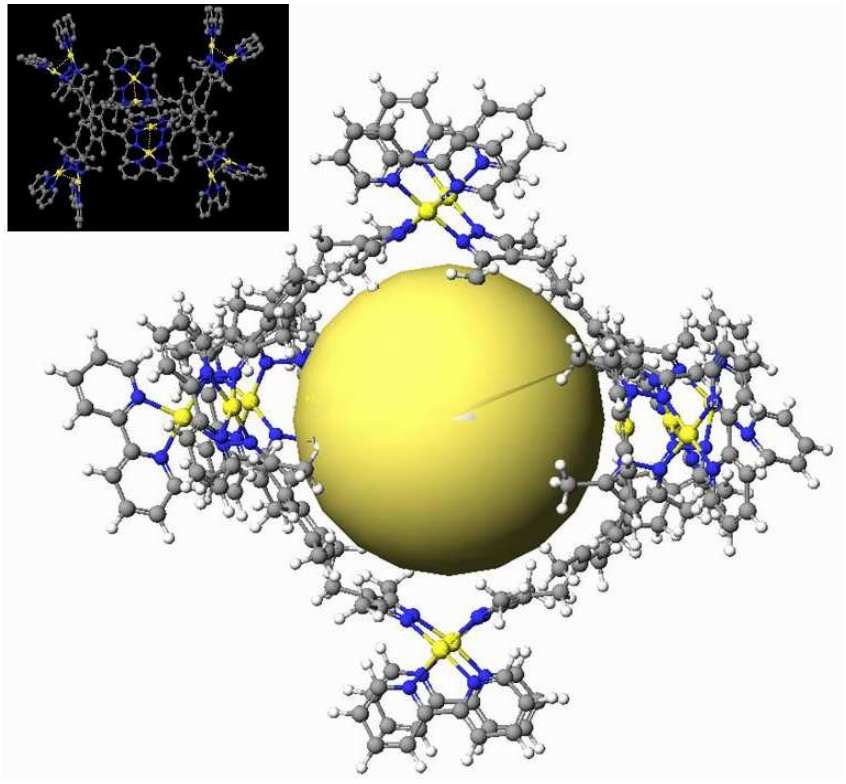

Figure 10. Ball-and-stick model of macrotricyclic cage **4a** computed with the CAChe program 6.1.1

program, insertion is the side view of **4a**. Yellow, Pd (II); gray, C; blue, N; pale, H. The central yellow ball is a pseudoatom).

In a similar fashion, complex **4b** was formed in high yield through the combination of dimetal clip $[(dmbpy)_2Pd_2(NO_3)_2](NO_3)_2$ with tripyrazole ligand H_3L^4 in the molar ratio of 3:1 in aqueous solution. The steric effect from the methyl groups of dmbpy ligands cause the different shape in comparing with **4a**. The ^1H and ^{13}C NMR spectra indicated the formation of a single product. As shown in the Figure S24 and S25, the ^1H NMR spectra revealed that complex **4b** possessing a highly distorted structure with a 10:4 complex of dimetal clip to L^4 is formed. The eight sets of signals appearing at 7.37 to 8.20 ppm in the downfield region were ascribed to protons of 4, 4′-dimethyl-2, 2′-bipyridine. Meanwhile, five sets of doublet observed at 4.31, 4.10, 3.79, 3.53, 3.21 ppm were ascribed to the protons of the methane groups (Ar-CH_2-). The chemical shifts found at 2.42 to 2.91 ppm were due to methyl groups (Ar-CH_3). The signals of methyl groups on the pyrazole were observed at 2.06, 1.75, 1.64 and 1.38 ppm. The formation of the **[**$Pd_{10}L^4_4]^{10+}$-type cage was further supported by cold electron spray ionization mass spectrometry (CSI-MS): 997.06 and 1262.49 for [**4b** • $5NO_3^-]^{5+}$ and [**4b** • $6NO_3^-]^{4+}$ (Figure S26).

After replacing dimetallic clips $[(bpy)_2Pd_2(NO_3)_2](NO_3)_2$ with $[(dmbpy)_2Pd_2(NO_3)_2](NO_3)_2$, a remarkable different assemble was yield. The experimental finding is that $[Pd_{10}L^4_4]$-Type trimacrocycle is formed. Single crystals of compound **4b** were obtained by slow evaporation of its aqueous solution. As shown in Figure 34, the crystal structure of compound **4b** also displays a $[Pd_{10}L^4_4]$ metal-organic trimacrocyclic structure, and the selected bond lengths and angles are depicted. Complex **4b** • $10NO_3$ crystallizes in the triclinic space group *P-1*. The crystal structure analysis for **4b** reveals the Pd_{10} highly distorted macrocycle-shaped structure with four (μ-pyrazolato-N, N′)$_2$ doubly-bridged $[(bpy)Pd]_2$ dimetal corners and two (bpy)Pd monometallic corners. The molecular dimensions are approximately 12 Å × 11 Å × 22 Å (i.e. the distances between the Pd(II) atoms of the $[(dmbpy)_2Pd_2(pz)_2]^{2+}$ coordination motifs). Like with **2a** and **2b**, two pyrazolate groups located at the 1 and 3-position of linker L^2 were locked by two $[(dmbpy)_2Pd_2(pz)_2]^{2+}$ coordination motifs, resulting in the formation of

$[Pd_4L^2_2]$ macrocyclic subunits bearing two intermolecular dimetal coordination motifs with Pd···Pd distances of 3.228 to 3.221 Å (Table S6). The dihedral angles between three pyrazolyl and backbone aromatic group are 71.18°, 83.75° and 87.50°, respectively. Two phenyl groups arranged in the almost plane, three pyrazolate groups adopted the favorable conformer in up, up, down mode. Two $[Pd_4L^4_2]$ macrocyclic subunits were hold together through two pyrazolate groups at the 5-position bridging-coordinate with single metal $[(bpy)Pd]^{2+}$ corners, finally leading to the construction of $[Pd_{10}L^4_4]^{10+}$ trimacrocyclic cage.

Conclusions.

We have synthesized a new class of rigid and flexible poly-pyrazole ligands *via* multi-step reaction on the backbone of benzenes. By using these functional tripyrazolate ligands, six novel metal-organic Pd-based supramolecular architectures including macrocycles and dimeric cages were designed and self-assembled from dipalladium corners and tripyrazole ligands through a directed self-assembly process that occurs along with spontaneous deprotonation of the ligands. These assemblies have been fully characterized by element analysis, ^{1}H and ^{13}C NMR, CSI-MS or ESI-MS and in the cases of **1-4** by single crystal X-ray diffraction methods. Because of the high stability in strong acidic aqueous solution, these metal-organic species with inter cavity have potential application in the field of molecular encapsulation, molecular catalysis and molecular reactor.

Experimental Section

Materials. All chemicals and solvents were of reagent grade and were purified according to conventional methods.[22] The dimetal clips $[(bpy)_2Pd_2(NO_3)_2](NO_3)_2$, $[(phen)_2Pd_2(NO_3)_2](NO_3)_2$ and $[(dmbpy)_2Pd_2(NO_3)_2](NO_3)_2$ were prepared according to literature procedures.[18]

X-ray Structural Determinations. X-ray diffraction measurements were carried out at 291 K on a Bruker Smart Apex CCD area detector equipped with a graphite monochromated MoKα radiation (λ= 0.71073 Å). The absorption correction for all complexes was performed using SADABS. All the

structures were solved by direct methods and refined employing full-matrix least-squares on F^2 by using SHELXTL (Bruker, 2000) program and expanded using Fourier techniques. All non-H atoms of the complexes were refined with anisotropic thermal parameters. The hydrogen atoms were included in idealized positions. Final residuals along with unit cell, space group, data collection, and refinement parameters are presented in Table 1.

CAChe Program 6.1.1: Two visual molecular models were computed using *CAChe* program 6.1.1[23] to evaluate shape of metallo-cages **4a** and **5**.

Scheme 4. Synthesis of tripyrazole ligands (**H_3L^4~ H_3L^5**)

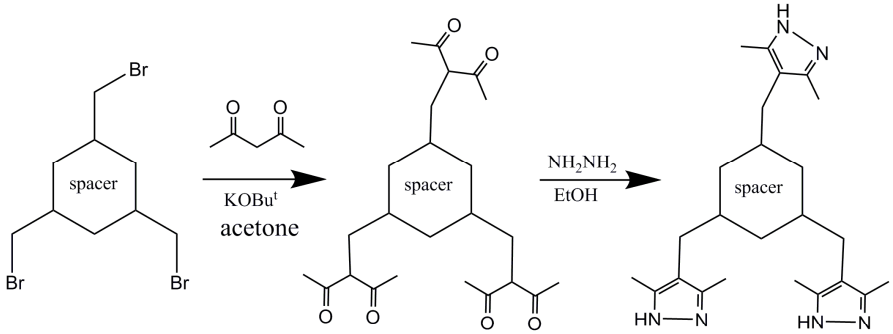

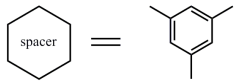

6 **H_3L^4**

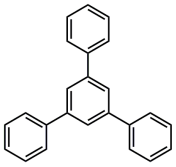

7 **H_3L^5**

General Tripyrazole Ligands Preparation. As shown in Scheme 4, all precursors were prepared according to reported methods.[16,17] Hydrazine hydrate (1 ml, 80%) was added during a 10-min period to a stirred, refluxing solution of dione (1 mmol) in 30 ml of ethanol. After 12 hours, most of the solvent was distilled and filtered, and the resulting solid was washed with water twice and vacuum dried.

Preparation of 1, 3, 5-tri(1*H*-pyrazol-3-yl)- benzene (H_3L^1). The tripyrazole ligand H_3L^1 was synthesized according to published methods.[21] ^{1}H NMR (400 MHz, DMSO-*d*6, 25°C, ppm): δ 11.98 (s, 3H, Pz-NH), 7.15 (s, phenyl-H), 6.73, 5.68 (d, J = 7.4 Hz, 6H, Pz-H). ^{13}C NMR (100 MHz, DMSO-*d*6, 25°C, ppm): δ158.47, 136.82, 131.3, 121.51, 102.78. Anal. Calcd. for $C_{15}H_{12}N_6$ (%):C, 65.21; H, 4.38;

N, 30.42; Found: C, 65.18; H, 4.35; N, 30.46.

Preparation of 1, 3, 5-tri((3, 5-dimethyl-1*H*-pyrazol-4-yl)methyl)-2, 4, 6-trimethyl benzene (H_3L^4). To a suspension of **6** in ethanol (50 ml) was added 3 ml of 80% aqueous solution of hydrazine hydrate The resulting mixture was refluxed for 5 hours, and then cooled to room temperature. The product was collected by filtration, washed with water twice and dried under vacuum (1.4g, 86%). Mp 264 °C. ^{1}H NMR (400 MHz, DMSO-*d*6, 25°C, ppm): δ 11.78 (s, 3H, NH), 3.67 (s, 6H, methyl-H), 2.07 (s, 9H, CH_3-Ar), 1.80 (s, 18H, CH_3-Pz). ^{13}C NMR (100 MHz, DMSO-*d*6, 25°C, ppm): δ134.1, 133.3, 111.2, 25.3, 16.4, 10.6. ESI-MS (DMSO, m/z): $[M+CH_3OH+H]^+$, calcd for $C_{28}H_{41}N_6O^+$; 478.66, found, 479.24. Elemental analyses calcd (%) for $C_{27}H_{36}N_6$: C, 72.94; H, 8.16; N, 18.90; Found: C, 71.98; H, 8.18; N, 18.84.

Preparation of 1, 3, 5-tri((3, 5-dimethyl-1*H*-pyrazol-4-yl)-methylphenyl)- benzene (H_3L^5). The above general tripyrazole ligands preparation procedure was followed except for the substitution of hydrazine hydrate (2 ml, 80%) and **7** (680 mg, 1.7 mmol) in 50ml of ethanol. Then the yellow solid **H_3L^5** was obtained. Yield: 630 mg (90%). Mp 251□. ^{1}H NMR (400 MHz, DMSO-*d6*, 25°C, ppm): δ 7.76 (s, 3H, NH), δ7.70-7.68 (d, *J* = 8.4 Hz, 6H, Ar-Pz), 7.22-7.20 (d, *J* = 8.4 Hz, 6H, phenyl-H), 3.71 (s, 6H, methyl-H), 2.09 (s, 18H, CH_3-Pz). ^{13}C NMR (100 MHz, DMSO-*d6*, 25°C, ppm): δ 141.4, 141.0, 137.6, 128.5, 127.0, 125.43113.2, 28.1, 10.7. ESI-MS (DMSO, m/z): $[M+H]^+$, calcd for $C_{42}H_{43}N_6^+$; 631.36, Found: 631.37. Elemental analyses calcd (%) for $C_{42}H_{42}N_6$: C, 79.97; H, 6.71; N, 13.32; Found: C, 79.98; H, 6.78; N, 13.34.

General Procedures. $\{[(bpy)Pd]_6L^1_2\}(PF_6^-)_6$ (**1**•6PF_6^-). Combination dimetal clips $[(bpy)_2Pd_2(NO_3)_2](NO_3)_2$ (39 mg, 0.1 mmol) with a suspension of **H_3L^1** (9.7 mg, 0.033 mmol) in H_2O (5 ml) and acetone (5 ml), and the mixture was stirred for 24 hours at 80°C. The resulting clear yellow solution was slowly evaporated to give a light yellow crystalline **1**•6NO_3^-. Yield: 41.2 mg (83 %).

The PF_6^- salt of **1** was obtained as yellow microcrystals in quantitative yield. ^{1}H NMR (400 MHz,

[D_3]CD_3CN, 25 °C, ppm) δ = 8.48-8.45 (t, *J* = 8.4 Hz, 12H, bpy-H), 8.41-8.44 (t, *J* = 8.8 Hz, 24H, bpy-H), 7.87 (m, 12H, bpy-H), 7.68 (d, 12H, *J* = 7.4 Hz, Pz-H), 7.52 (s, 6H, Ar-H); ^{13}C NMR (100 MHz, CD_3CN, 25°C, ppm): δ158.45, 156.39, 153.06, 145.35, 142.34, 131.88, 129.46, 128.07, 124.15, 123.61, 105.46, 29.97. CSI-MS (acetonitrile, *m/z*): 1350.3，852.2，602.7, 453.3 and 353.5 for [**1**•4PF_6^-]$^{2+}$, [**1**•3PF_6^-]$^{3+}$, [**1**•2PF_6^-]^{4}, [**1**•PF_6^-]$^{5+}$ and [**1**]$^{6+}$. Elemental analyses calcd (%) for $C_{90}H_{78}F_{36}N_{24}O_6P_6Pd_6 \cdot 6H_2O$: C, 34.87; H, 2.54; N, 10.84; Found: C, 34.81; H, 2.58; N, 10.87.

{[(bpy)Pd]$_{10}$L$^2_4$}(NO$_3^-$)$_{10}$ (2a•10NO_3^-**):** [$(bpy)_2Pd_2(NO_3)_2$]$(NO_3)_2$ (0.0385 mg, 0.1 mmol) was added to a suspension solution of **H_3L^2** (0.01 mg, 0.033 mmol) in H_2O/acetone. The mixture was stirred at 80 °C for 48 hours until orange precipitate completely disappeared, then all solvent removed under vacuum and leading to the formation of positively charged metallomacrocycles [$Pd_{10}L^2_4$]$(NO_3^-)_{10}$ as a pale yellow precipitate. The crystalline sample of **2a**•10NO_3^- was obtained by evaporation of water at room temperature in the yield of 89%. The related PF_6^- salts were prepared by anion exchange with a 10-fold excess of KPF_6, respectively. The ^{1}H NMR analysis clearly indicated the formation of a single product. Complex **2a**•10NO_3^-: ^{1}H NMR (400 MHz, D_2O/CD_3COCD_3, 25℃): δ = 8.78~8.35 (m, 64H, bpy-H), 7.91~7.62 (m, 16H, bpy-H), 7.45, 6.24 and 6.31 (s, 12H, Ar-H), 2.81, 2.67, 2.52 and 1.58 (s, 72H, CH_3-Pz). ^{13}C NMR (100 MHz, CD_3CN, 25°C, ppm): δ156.11, 155.23, 148.94, 145.08, 140.17, 132.41, 126.52, 121.29, 118.63, 113.35, 13.74, 12.88, 11.21, 10.08, 9.87. ESI-MS(CH_3OH, *m/z*): 1107.6， 873.1 and 717.6 for [**2a** • 6NO_3^-]$^{4+}$, [**2a** • 5 NO_3^-]$^{5+}$ and [**2a** • 4NO_3^-]$^{6+}$. Elemental analyses calcd (%) for $C_{184}H_{166}N_{54}O_{30}Pd_{10} \cdot 5H_2O$: C, 46.35; H, 3.72; N, 15.86; Found: C, 46.25; H, 3.68; N, 15.79.

{[(dmbpy)Pd]$_{10}$L$^2_4$}(NO$_3^-$)$_{10}$ (2b•10NO_3^-**):** The same procedure for **2a** was using to prepare cage **2b** except the dimetal clip. ^{1}H NMR (400 MHz, D_2O/CD_3COCD_3, 25℃): δ = 8.40~8.10 (m, 40H, dmbpy-H), 7.86~7.39 (m, 20H, dmbpy-H), 7.33, 6.60 and 6.28 (s, 12H, Ar-H), 2.71, 2.54, 2.49 and 2.42 (m, 60H, CH_3-dmbpy), 2.61, 1.64, 1.49 (s, 72H, CH_3-dmbpy). ^{13}C NMR (100 MHz, DMSO-d6, 25°C, ppm): δ157.31, 154.82, 151.23, 148.53, 148.11, 143.08, 134.51, 127.43, 123.08, 25.53, 24.27, 20.07,

17.67, 14.56, 12.63, 11.27, 9.56. CSI-MS (methanol, *m/z*): 764.04 [**2b** • $4NO_3^-$]$^{6+}$, 929.55 [**2b** • $5NO_3^-$]$^{5+}$, 1177.36 [**2b** • $6NO_3^-$]$^{4+}$. Elemental analyses calcd (%) for $C_{204}H_{204}N_{54}O_{30}Pd_{10}\cdot 2H_2O$: C, 49.08; H, 4.20; N, 15.15; Found: C, 49.11; H, 4.28; N, 15.19.

{[(phen)Pd]$_{12}$L$^3_4$}(PF$_6^-$)$_{12}$ (**3**•12PF6$^-$). The above general procedure was followed except for substitution of $[(bpy)_2Pd_2(NO_3)_2](NO_3)_2$ (39 mg, 0.1 mmol) with **H$_3$L^3** (13.8 mg, 0.033 mmol) and the resulting clear yellow solution was evaporated to dryness to give a yellow solid **3** • $12NO_3^-$. Yield: 51 mg (95%). The PF_6^- salt of **3** was obtained as yellow microcrystals in quantitative yield. ^{1}H NMR (400 MHz, CD_3CN, 25 ^{o}C, ppm) δ = 8.87(d, *J* = 8.4 Hz, 12H, phen-H), 8.78 (d, *J* = 8.4 Hz, 12H, phen-H), 8.38 (t, *J* = 8.4 Hz, 24H, phen-H), 8.18 and 8.11 (s, 24H, phen-H), 7.95 (m, 24H, phen-H), 7.66 and 5.79 (s, 12H, Ar-H), 4.01 and 3.87 (d, *J* = 8.8 Hz, 24H, $ArCH_2$-H), 2.71, 2.22 and 2.02 (s, 72H, $PzCH_3$-H). ^{13}C NMR (100 MHz, CD_3CN, 25°C, ppm): δ 159.31, 158.67, 154.24, 153.17, 152.23, 143.14, 138.83, 133.31, 128.72, 124.33, 123.86, 119.60, 21.07, 19.63, 14.18, 11.71, 9.81. ESI-MS (acetonitrile, *m/z*): 1209.8 [**3** • $7PF_6^-$]$^{5+}$, 984.5 [**3** • $6PF_6^-$]$^{6+}$, 823.0 [**3** • $5PF_6^-$]$^{7+}$, 702.1 [**3** • $4PF_6^-$]$^{8+}$, 608.0 [**3** • $3PF_6^-$]$^{9+}$. Elemental analyses calcd (%) for $C_{237}H_{201}F_{84}N_{47}P_{14}Pd_{12}\cdot 5CH_3CN$: C, 41.19; H, 3.01; N, 10.07; Found: C, 41.13; H, 3.10; N, 10.11.

{[(bpy)Pd]$_{12}$L$^4_4$}(PF$_6^-$)$_{12}$ (**4a**•12PF$_6^-$). The above general procedure was followed except for substitution of $[(bpy)_2Pd_2(NO_3)_2](NO_3)_2$ (39 mg, 0.1 mmol) with **H$_3$L^4** (14.8 mg, 0.033 mmol) and the resulting clear yellow solution was evaporated to dryness to give a yellow solid **4a**•$12NO_3^-$. Yield: 51 mg (95%). The PF_6^- salt of **4a** was obtained as yellow microcrystals in quantitative yield. ^{1}H NMR (400 MHz, CD_3CN, 25 ^{o}C, ppm) δ = 8.57-8.36 (m, 48H, bpy-H), 8.26 and 7.57 (t, *J* = 8.4 Hz, 24H, bpy-H), 8.03 and 7.95 (m, 24H, bpy-H), 4.26-3.29 (m, 12H, $ArCH_3$-H), 2.58 (d, *J* = 12.4 Hz, 12H, $ArCH_3$-H), 2.18-2.12 (d, *J* = 10.4 Hz, 12H, $ArCH_3$-H) 1.81-1.69 (s, 48H, $PzCH_3$-H), 1.44 (s, 12H, $PzCH_3$-H). ^{13}C NMR (100 MHz, CD_3CN, 25°C, ppm): δ 156.56, 151.2, 150.64, 148.22, 143.24, 142.83, 134.55, 133.37, 128.29, 127.91, 124.35, 123.83, 115.80, 29.98, 25.39, 16.40, 11.81, 9.58. ESI-MS (acetonitrile, *m/z*): 1519.2 [**4a** • $8PF_6^-$]$^{4+}$, 964.3 [**4a** • $6PF_6^-$]$^{6+}$. Elemental analyses calcd (%) for $C_{228}H_{228}F_{72}N_{48}P_{12}Pd_{12}$: C,

41.14; H, 3.45; N, 10.10; Found: C, 41.12; H, 3.41; N, 10.16.

{[(dmbpy)Pd]$_{10}$L$^4_4$}(NO$_3^-$)$_{10}$ (4b•10NO$_3^-$). In a similar fasion, compound **4b** was formed through the combination of dimetal clip [(dmbpy)$_2$Pd$_2$(NO$_3$)$_2$](NO$_3$)$_2$ (41 mg, 0.1 mmol) with **H$_3$L^4** (14.8 mg, 0.033 mmol). Pure **4b** as a crystalline yellow solid was obtained by the vapor diffusion of diethyl ether into a soltuion of **4b** in methanol at room temperature. Yield: 54.8 (98%). ^{1}H NMR (400 MHz, CD$_3$COCD$_3$/D$_2$O, 25 ^{o}C, ppm) δ = 8.20-7.98 (m, 30H, dmbpy-H), 7.77-7.38 (m, , 30H, dmbpy-H), 4.27, 4.10, 3.79, 3.17, 2.91 (d, *J* = 10.4 Hz, 24H, Ar-CH$_2$-Pz), 2.91-2.42 (m, 96H, ArCH$_3$-H and dmbpy-CH$_3$-H), 2.16, 1.76, 1.64, 1.38 (s, 72H, PzCH$_3$-H). ^{13}C NMR (100 MHz, CD$_3$CN, 25°C, ppm): δ 156.04, 155.56, 154.93, 152.37, 149.94, 136.72, 128.26, 124.46, 20.70, 18.21, 17.45, 11.77. CSI-MS (methanol, *m/z*): 997.06 [**4b** • 5NO$_3^-$]$^{5+}$, 1262.49 [**4b** • 6NO$_3^-$]$^{4+}$. Elemental analyses calcd (%) for C$_{228}$H$_{252}$N$_{54}$O$_{30}$Pd$_{10}$ •2H$_2$O: C, 51.39; H, 4.84; N, 14.19; Found: C, 51.32; H, 4.78; N, 14.16.

{[(bpy)Pd]$_6$L$^5_2$}(PF$_6^-$)$_6$ (5 • 6PF$_6^-$). The above general procedure was followed with **H$_3$L^5** (34.7 mg, 0.033 mmol); the resulting clear yellow solution was evaporated to dryness to give a yellow solid **5** • 6NO$_3^-$. Yield: 57 mg (80%). The PF$_6^-$ salt of **5** was obtained by adding a ten-fold excess of KPF$_6$ to its aqueous solution at 60°C, which resulted in the immediate deposition of **5** • 6PF$_6^-$ as yellow microcrystals in quantitative yield. ^{1}H NMR (400 MHz, CD$_3$CN, 25 ^{o}C, ppm) δ = 8.85 (t, *J* = 8.4 Hz , 12H, bpy-H$_\delta$), 8.74 (d, *J* = 8.4 Hz , 12H, bpy-H$_\gamma$), 8.48 (t, *J* = 8.4 Hz, 12H, bpy-H$_\alpha$), 8.17 (d, *J* = 8.4 Hz 12H, bpy-H$_\beta$), 7.59-7.57 (m, 24H, Ar-H), 7.35 (m, 6H, Ar-H), 4.25 (s, 12H, Ar-*CH$_2$*), 2.44 (s, 36H, Pz-CH$_3$). ^{13}C NMR (100 MHz, CD$_3$CN, 25°C, ppm): δ153.1, 152.8, 152.5, 150.4, 148.7, 148.5, 142.7, 142.3, 132.2, 129.1, 123.2, 114.3, 82.2, 31.2, 26.2, 15.5. ESI-MS (acetonitrile, *m/z*): 1090.3、586.2 and 472.7 for [**5** • 3PF$_6^-$]$^{3+}$, [**5** • PF$_6^-$]$^{5+}$, [**5**]$^{6+}$. Elemental analyses calcd (%) for C$_{144}$H$_{138}$F$_{36}$N$_{24}$P$_6$Pd$_6$ •CH$_3$CN: C, 46.71; H, 3.79; N, 9.33; Found: C, 46.68; H, 3.78; N, 9.36.

Acknowledgement. This project was supported by National Natural Science Foundation of China (No. 20772152). This work was supported by National Natural Science Foundation of China (No. 91127039,

51073171), Beijing Natural Science Foundation (No.2112018), and the Research Funds of Renmin University of China (No. 11XNL011) and BSRF for The crystal structure determination using synchrotron radiation X-ray diffraction analysis. We are also grateful to Prof. Dr. Yizhi Li in Nanjing University for the X-ray crystallography.

Reference:

1 (a) F. A. Cotton, R. A. Walton, *Multiple Bonds Between Metal Atoms*; Oxford University Press: Oxford, 1993. (b) F. A. Cotton, C. A. Murillo, R. A. Walton, *Multiple Bonds Between Metal Atoms*, 3rd ed.; Springer Science and Business Media, Inc.: New York, **2005**.

2 G. B. Kauffman (Ed.), *Coordination Chemistry:* A *Century of Progress*, vol. 565, American Chemical Society, Washington, DC, **1994**.

3 J.-M. Lehn, *Supramolecular Chemistry, Concepts and Perspectives*; VCH: Weinheim, Germany, **1995**.

4 (a) C. J. Ballhausen, *Introduction to Ligand Field Theory*; McGraw Hill: New York, 1962. (b) J. D. Atwood, M. J. Wovkulich, D. C. Sonnenberger, *Acc. Chem. Res.* **1983**, *16*, 350-355.

5 (a) F. A. Cotton, C. Lin, C. A. Murillo, *Acc. Chem. Res.* **2001**, *34*, 759-771. (b) H. Chifotides, K. R. Dunbar, *Acc. Chem. Res.* **2005**, *38*, 146-156.

6 (a) J.-P. Sauvage, *Transition Metals in Supramolecular Chemistry, Perspectives in Supramolecular Chemistry*; Wiley: New York, **1999**; Vol. 5. (b) M. Fujita, *Molecular Self-Assembly Organic Versus Inorganic Approach (Structure and Bonding)*; Springer: New York, **2000**; Vol. 96. (c) D. L. Caulder, K. N. Raymond, *Acc. Chem. Res.* **1999**, 32, 975-982. (d) J. A. R. Navarro, B. Lippert, *Coord. Chem. Rev.* **1999**, *185-186*, 653-667. (e) M. Fujita, M. Tominaga, A. Hori, B. Therrien, *Acc. Chem. Res.* **2005**, *38*, 371-380. (f) F. Würthner, C.-C. You, C. R. Saha-Möller, *Chem. Soc. Rev.* **2004**, *33*, 133-146. (g) S. R.

Seidel, P. J. Stang, *Acc. Chem. Res.* **2002**, *35*, 972-983.

7 (a) G. La Monica, G. A. Ardizzoia, In *Progress in Inorganic Chemistry*, K. D. Karlin, Ed.; Wiley: New York, **1997**; Vol. 46, pp 151-238; (b) S. Trofimenko, In *Progress in Inorganic Chemistry*, S. J. Lippard, Ed.; Wiley: New York, **1986**; Vol.34, pp 115-206; (c) S. Trofimenko, *Chem. Rev.* **1972**, *72*, 497-509; (d) S.-Y. Yu, S.-H. Li, H.-P. Huang, Z.-X. Zhang, Q. Jiao, H. Shen, X.-X. Hu, H. Huang, *Curr. Org. Chem.* **2005**, *9*, 555-563.

8 (a) C. F. Martens, R. J. M. Klein Gebbink, M. C. Feiters, R. J. M. Nolte, *J. Am. Chem. Soc.* **1994**, *116*, 5667-5670; (b) Togni, A.; Burckhardt, U.; Gramlich, V.; Pregosin, P. S.; Salzmann, R. *J. Am. Chem. Soc.* **1996**, *118*, 1031-1037; (c) A. L. Dearden, S. Parsons, R. E. P. Winpenny, *Angew. Chem. Int. Ed.* **2001**, *40*, 152-154; (d) J.-P. Zhang, S. Kitagawa, *J. Am. Chem. Soc.* **2008**, *130*, 907.

9 (a) S. J. Dougan, M. Melchart, A. Habtemariam, S. Parsons, P. J. Sadler, *Inorg. Chem.* **2006**, *45*, 10882-10894; (b) D. L. Banville, L. G. Marzilli, *Biochemistry* **1986**, *25*, 7393-7401.

10 (a) A. Das, K. Gieb, Y. Krupskaya, S. Demeshko, S. Dechert, R. Klingeler, V. Kataev, B. Büchner, P. Müller, F. Meyer, *J. Am. Chem. Soc.* **2011**, *133*, 3433–3443; (b) O. Stefanczyk, T. Korzeniak, W. Nitek, M. Rams, B. Sieklucka, *Inorg. Chem.* **2011**, *50*, 8808–8816; (c) G. N. Newton, T. Onuki, T. Shiga, M. Noguchi, T. Matsumoto, S. J., M. M. Nihei, M. Nakano, L. Cronin, H. Oshio,*Angew. Chem. Int. Ed.* **2011**, *50*, 4844-4846.

11 (a) A. C. Jahnke, K. Pröpper, C. Bronner, J. Teichgräber, S. Dechert, M. John, O. S. Wenger, F. Meyer, *J. Am. Chem. Soc.* **2012**, *134*, 2938−2941; (b) B. Ma, J. Li, P. I. Djurovich, M. Yousufuddin, R. Bau, M. E. Thompson, *J. Am. Chem. Soc.* **2005**, *127*, 28-29; (c) W. Lu, M. C. W. Chan, N. Zhu, C.-M. Che, C. Li, Z. Hui, *J. Am. Chem. Soc.* **2004**, *126*, 7639-7651; (d) S.-W. Lai, M. C.-W. Chan, T.-C. Cheung, S.-M. Peng, C.-M. Che, *Inorg. Chem.* **1999**, *38*, 4046-4055; (e) S.-W. Lai, M. C.-W. Chan, T.-C. Cheung, S.-M. Peng, C.-M. Che, *Organometallics* **1999**, *18*, 3991-3997; (f) A. Kishmura, T.

Yamshita, T. Aida, *J. Am. Chem. Soc.* **2005**, *127*, 179-183; (g) M. Enomoto, A. Kishimura, T. Aida, *J. Am. Chem. Soc.* **2001**, *123*, 5608-5609; (h) A. A. Mohamed, A. Burini, J. P. Fackler, *J. Am. Chem. Soc.* **2005**, *127*, 5012.

12 (a) V. W.-W. Yam, K.-L. Yu, K.-K. Cheung, *Dalton Trans.* **1999**, 2913; (b) V. W.-W. Yam, K. M.-C. Wong, N. Zhu, *J. A*m. Chem. Soc**. 2002**, *124*, 6506-6507; (c) V. W.-W. Yam, C.-K. Hui, S.-Y. Yu, N.-Y. Zhu, *Inorg. Chem.* **2004**, *43*, 812-821; (d) J. P. H. Charmant, J. Forniés, J. Gómez, E. Lalinde, R. I. Merino, M. T. Moreno, A. G. Orpen, *Organometallics* **1999**, *18*, 3353-3358; (e) I. Ara, J. Fornie´s, J. Gómez, E. Lalinde, M. T. Moreno, *Organometallics* **2000**, *19*, 3137-3144; (f) J. Forniés, S. Fuertes, A. Martín, V. Sicilia, E. Lalinde, M. T. Moreno, *Chem.–Eur. J.* **2006**, *12*, 8253.

13 (a) K.-B. Shiu, H.-C. Lee, G.-H. Lee, B. T. Ko, Y. Wang, C.-C. Lin, *Angew. Chem., Int. Ed.* **2003**, *42*, 2999-3001; (b) K.-B. Shiu, H.-C. Lee, G.-H. Lee, Y. Wang, *Organometallics* **2002**, *21*, 4013-4016; (c) G. Süss-Fink, J.-L. Wolfender, F. Neumann, H. Stoeckli-Evans, *Angew. Chem., Int. Ed. Engl.* **1990**, *29*, 429-431; (d) J.-P. Zhang, S. Kitagawa, *J. Am. Chem. Soc.***2008***, 130*, 907-917; (e) G. Yang, R. G. Raptis, *Inorg. Chem.* **2003**, *42*, 261-263; (f) H. V. R. Dias, H. V. K. Diyabalanage, M. G. Eldabaja, O. Elbjeirami, M. A. Rawashdeh-Omary, M. A. Omary, *J. Am. Chem. Soc.* **2005**, *127*, 7489-7501; (g) M. A. Omary, M. A. Rawashdeh-Omary, M. W. A. Gonser, O. Elbjeirami, T. Grimes, T. R. Cundari, *Inorg. Chem.* **2005**, *44*, 8200-8210; (h) H. V. R. Dias, C. S. P. Gamage, *Angew. Chem., Int.Ed.* **2007**, *46*, 2192-2194; (i) A. Hayashi, M. M. Olmstead, S. Attar, A. L. Balch, *J. Am. Chem. Soc.* **2002**, *124*, 5791-5795; (j) C. Burress, O. Elbjeirami, M. A. Omary, F. P. GabbaÏ, *J. Am. Chem. Soc.* **2005**, *127*, 12166-12167.

14 (a) H.-P. Huang, S.-H. Li, S.-Y. Yu, Y.-Z. Li, Q. Jiao, Y.-J. Pan, *Inorg. Chem. Commun.* **2005**, *8*, 656-660; (b) K. Umakoshi, Y. Yamauchi, K. Nakamiya, T. Kojima, M. Yamasaki, H. Kawano, M. Onishi, *Inorg. Chem.* **2003**, *42*, 3907-3916; (c) A. Boixassa, J. Pons, X. Solans, M. Font-Bardia, J. Ros, *Inorg. Chem. Commun.* **2003**, *6*, 922-925; (d) J. Pons, A. Chadghan, J. Casabo´, A. Alvarez-Larena,

J. F. Piniella, J. Ros, *Inorg. Chem. Commun.* **2000**, *3*, 296-299; (e) K. Sakai, T. Sato, T. Tsubomura, K. Matsumoto, *Acta Crystallogr., Sect. C* **1996**, *52*, 783-786.

15 (a) Z. X. Zhang, H. Huang, S.-Y. Yu, *Chin. J. Inorg. Chem.* **2004**, *20*, 849; (b) S.-Y. Yu, H. P. Huang, S. H. Li, Q. Jiao, Y. Z. Li, B. Wu, Y. Sei, K. Yamguchi, Y. J. Pan, H. W. Ma, *Inorg. Chem*. **2005**, *44*, 9471-9488.

16 (a) J. Tong, S.-Y. Yu, H. Li, *Chem. Commun.* **2012**, *48*, 5343-5345; (b) S. H. Li, H. P. Huang, S.-Y. Yu, X.-P. Li, *Chinese Journal of Chemistry*, **2006**, *24*, 1225-1229; (c) Q. F. Sun, K. M.-C. Wong, L. X. Liu, H.-P. Huang, S.-Y. Yu, V. W.W. Yam, Y. Z. Li, Y. J. Pan, K. C. Yu, *Inorg. Chem.* **2008**, *47,* 2142–2154; (d) G. H. Ning, L.Y. Yao, L. X. Liu, T.-Z. Xie, Y.-Z. Li, Y. Qin, Y. J. Pan, S. Y. Yu, *Inorg. Chem.* **2010**, 49, 7783-7792; (e) L. Qin, L. Y. Yao, S.-Y. Yu, Inorg. Chem. **2012**, *51*, 2443-2453; (e) L. Y. Yao, Z. S. Yu, L. Qin, Y. Z. Li, Y. Qin, S. Y. Yu, *Dalton Trans.,* **2013**, 3447-3454.

17 (a) S. Y. Yu, Q. Jiao, S. H. Li, H. P. Huang, Y. Z. Li, Y. Sei, K. Yamaguchi, *Org. Lett.* **2007**, *9*, 1379-1382.

18 S. Y. Yu, M. Fujita, K. Yamaguchi, *J. Chem. Soc., Dalton. Trans.* **2001**, 3145-3146.

19 (a) K. Yamaguchi, *J. Mass Spectrom.* **2003**, *38*, 473; (b) S. Sakamoto, M. Fujita, K. Kim, K. Yamaguchi, Tetrahedron, **2000**, *56*, 955.

20 A.-K. Pleier, H. Glas, M. Grosche, P. Sirsch, W. R. Thiel, *Synthesis.* **2001**, *1*, 55.

21 W. L. F. Armarego, D. D. Perrin, *Purification of Laboratory Chemicals*, 4th ed; Butterworth Heinemann; Oxford, **1997**.

22 R. C. Conrad, J. V. Rund, *Inorg. Chem*. **1972**, *11*, 129.

23 CAChe 6.1.1 for Windows, Fujitsu Ltd., Chiba, Japan, **2003**.

24 A. W. Maverick, S. C. Buckingham, Q. Yao, J. R. Bradbury, G. G. Stanley, *J. Am. Chem. Soc.* **1986,**

108, 7430.

25 CCDC 1007897 (**1**•$6NO_3$), 1007898 (**2b**•$10NO_3$), 1007900 (**2a**•$10NO_3$), 1007899 (**3**•$12PF_6$) and 1007901 (**4b**•$10NO_3$) contain the supplementary crystallographic data for this paper. These data can be obtained free of charge from The Cambrige Crystallographic Data Centre via www.ccdc.cam.ac.uk/data_request/cif.